**Proceedings of the ASME 2022**
**Pressure Vessels & Piping Conference**
**PVP2022**
**July 17-22, 2022, Las Vegas, NV, USA**

**PVP2022-84514**

# SPECIMEN SIZE AND GEOMETRY EFFECTS ON THE MASTER CURVE FRACTURE TOUGHNESS MEASUREMENTS OF EUROFER97 AND F82H STEELS[a]

**Xiang (Frank) Chen[1], Mikhail A. Sokolov[1], Sehila M. Gonzalez De Vicente[2], Yutai Katoh[1]**
[1]Materials Science and Engineering Division, Oak Ridge National Laboratory
Oak Ridge, TN 37830, USA
[2]International Atomic Energy Agency, 1400 Vienna, Austria

[1] Contact author: chenx2@ornl.gov

## ABSTRACT

*EUROFER97 and F82H are two leading reduced-activation ferritic-martensitic (RAFM) steels for fusion blanket applications. Exposure to the harsh environment of fusion reactors can result in severe degradation of materials fracture toughness (FT). Thus, the post-irradiation evaluation of FT is critical to understanding the material behavior. Due to the space constraint of irradiation facilities, the development of small specimen test techniques (SSTT) is necessary to evaluate the performance of irradiated materials. In this study, we evaluated the specimen size and geometry effects on the ductile-to-brittle transition FT of EUROFER97 batch-3 and F82H-BA12 steels. The specimen thicknesses ranged from 1.65 to 12.7 mm and the geometries included 1.65 mm bend bar, 4 mm mini-compact tension (miniCT), and 0.5T compact tension (CT) specimens. Fracture toughness testing and evaluations were performed using the Master Curve method in the ASTM E1921-19 standard. After size correction to 1T size using the Master Curve method, no specimen size effect was observed between the 4 mm miniCT and 0.5T CT specimens for the Master Curve reference temperature $T_{0Q}$, while the bend bars yielded a higher $T_{0Q}$. A strong effect of fatigue precrack front straightness on $T_{0Q}$ for 0.5T CT specimens was observed. The minimum number of specimens needed for each specimen geometry has been determined.*

Keywords: EUROFER97, Fracture Toughness, Fusion, F82H, Master Curve, Small Specimen Test Techniques, Specimen Size Effect

## 1. INTRODUCTION

Reduced-activation ferritic-martensitic (RAFM) steel is the candidate structural material for fusion blanket applications [1-5]. Different countries have developed their version of reference RAFM steel, e.g., EUROFER97 for Europe and F82H for Japan. Both steels have favorable properties for fusion applications, such as reduced activation, superior swelling resistance, good thermal conductivity, and favorable fracture toughness (FT) in the normalized and tempered condition. However, exposing materials to the harsh environment of a fusion reactor, characterized by 14 MeV neutrons, will damage materials microstructure and produce transmutation products, such as n He/H [6], which can result in significant degradation of materials FT. Therefore, the post-irradiation evaluation of the FT of RAFM steels is critical to ensure the safe long-term operation of a fusion reactor [7]. Due to the space constraint of existing and future irradiation facilities, the development of small specimen test techniques (SSTT) is necessary to evaluate the performance of irradiated materials. Under the auspices of the International Atomic Energy Agency (IAEA), a Coordinated Research Project (CRP) entitled "Towards the Standardization of Small Specimen Test Techniques for Fusion Applications" has been ongoing since 2017. The overall objective of the project is to provide a set of guidelines for SSTT based on commonly agreed best practices for main test techniques including tensile, creep, low cycle fatigue, FT, and fatigue crack growth rate. The project will act as the first step towards a full standardization of SSTT for testing and qualifying fusion structural materials. As one participant in this project, Oak Ridge National Laboratory took a leading role in FT testing based on the Master Curve method described in the ASTM E1921-19 standard [8]. This paper summarizes our key findings concerning specimen size and geometry effects on Master Curve FT characterization for EUROFER97 and F82H steels.

## 2. MATERIALS AND METHODS

### 2.1 Materials and Specimens

Two plate materials of EUROFER97 batch-3 (heat 33307/07-097) and F82H-BA12 were used in FT testing. The compositions of both steels are shown in Table 1. The heat treatment for EUROFER97 batch-3 was austenitization at 980–1040°C for 27–30 min, followed by tempering at 750–760°C for 90–120 min [9]. The heat treatment for F82H-BA12 was standard normalization (1040°C for 40 min/air cooling) and tempering (750°C for 60 min/air cooling).

**Table 1** Compositions of EUROFER97 batch-3 [10] and F82H-BA12 (wt%)

| | Cr | C | Mn | V | W | Ta | Si | O | N |
|---|---|---|---|---|---|---|---|---|---|
| **E97** | 9.47 | 0.10 | 0.48 | 0.21 | 1.14 | 0.11 | 0.03 | 0.0012 | 0.0395 |
| **F82H** | 7.88 | 0.10 | 0.45 | 0.19 | 1.78 | 0.09 | 0.10 | 0.0012 | 0.0098 |

Three types of specimens, 0.5T compact tension (CT), 4 mm mini-compact tension (miniCT), and 1.65 mm bend bars, were machined from the middle thickness of two plates of EUROFER97 batch-3 and F82H-BA12 [11]. The specimen drawings are shown in Fig. 1. All specimens were machined in L-T orientation, i.e., with the crack plane normal to the rolling direction of the raw material and with the crack propagation parallel to the transverse direction of the raw material. It is worth noting that the material inhomogeneity could also affect the FT results, however, that is out of scope for this manuscript and since all specimens were machined close to each other, it is reasonable to believe that material inhomogeneity, if existing, does not apply in this work.

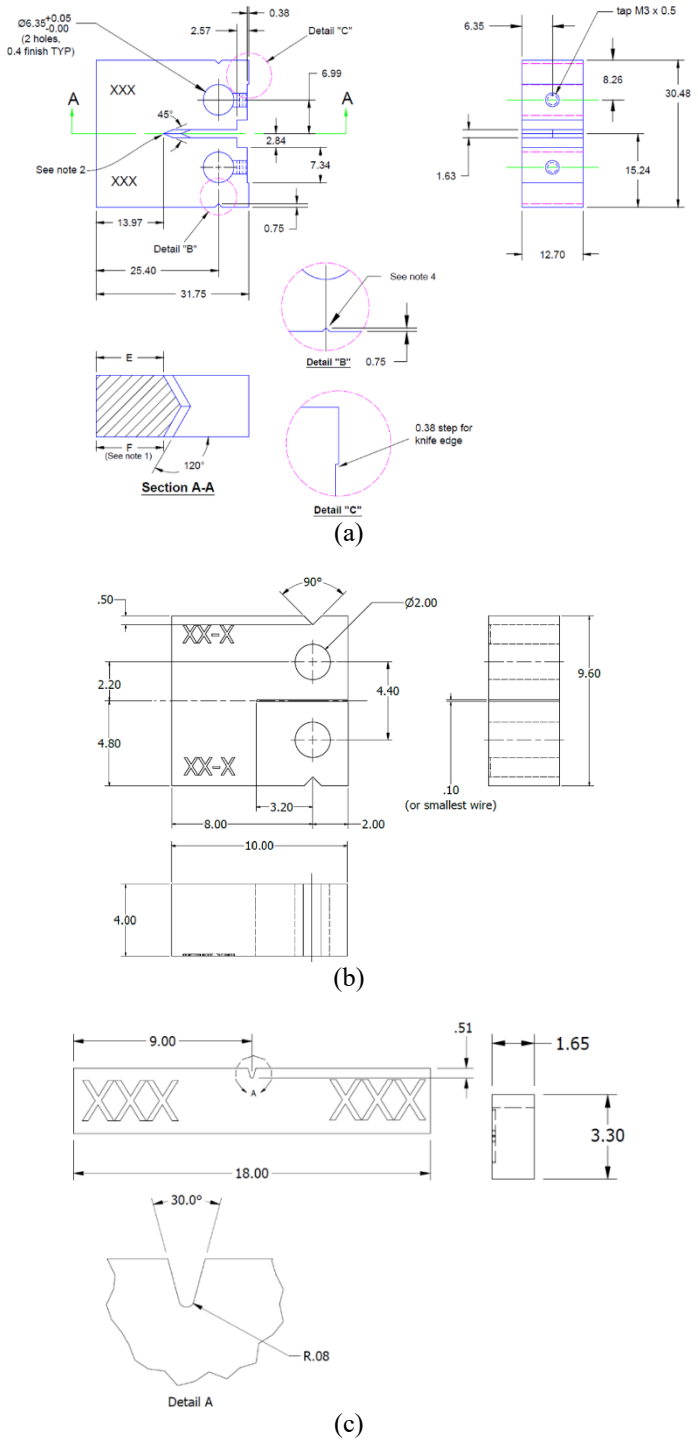


**FIGURE 1:** Specimen drawings for 0.5T CT in (a), 4 mm miniCT in (b), and 1.65 mm bend bar in (c). Dimensions in mm

### 2.2 Fracture Toughness Testing Equipment and Method

A detailed description of the testing equipment has been provided previously [11-16] and is briefly summarized here. Testing consisted of two parts: fatigue precracking and FT testing. Fatigue precracking was performed on a 44.5 kN capacity servo-hydraulic frame with calibrated load cells. Depending on the specimen geometry, dedicated fixtures, grips, and deflection gauges were used for each specimen type. A commercial automated fatigue crack growth testing software was used with real-time compliance-based crack size measurement to control the fatigue precrack process. FT testing was performed on a 97.87 kN capacity servo-hydraulic frame with calibrated load cells. Depending on the specimen geometry, dedicated fixtures, grips, and deflection gauges were used for each specimen type. Liquid nitrogen was used to control the testing temperatures, which were measured directly from type-T thermocouples spot welded to specimens. An environmental chamber was used to enclose specimens and the test fixture to ensure that the testing temperatures were within the ±2.5°C range from the target testing temperature.

Specimens were first fatigue precracked to the target crack size and then tested based on the Master Curve method described in the ASTM E1921-19 standard [8]. Specimens were not side-grooved. Fatigue cycling was conducted using a high frequency sinusoidal waveform under stress intensity factor K control with the fatigue stress ratio R = 0.1. For 0.5T CT and 4 mm miniCT specimens, a decreasing K was used while for 1.65 mm bend bars, a constant K was used. Per ASTM E1921, the following requirements were evaluated and satisfied during fatigue precracking:

- The applied stress intensity was within the envelope of allowable maximum stress intensity factor $K_{max}$
- The initial maximum fatigue force $P_{max}$ was less than the control force $P_m$
- Crack extension and final crack size requirements were met with fatigue precrack length $a_0/W \approx 0.5$.

FT testing was performed using a quasi-static loading rate such that dK/dt during the initial elastic loading portion was between 0.1 and 2 MPa√m/s. Testing temperatures were chosen such that the median stress intensity factor $K_{Jc(med)}$ at the test temperature was about 100 MPa√m for the specimen size selected. For 1.65 mm bend bar specimens, this was not possible due to the small FT capacity ($K_{Jclimit}$) inherent to the specimen type. Hence, lower testing temperatures had to be selected.

Each specimen was tested until either cleavage occurred or the displacement gauge travel limit was reached. Then the crack size was measured from the fracture surface. The equivalent elastic-plastic stress intensity factor $K_{Jc}$ was derived from the J-integral at the onset of cleavage fracture, $J_c$, using:

$$K_{Jc} = \sqrt{J_c \frac{E}{1-\nu^2}} \quad (1)$$

and then the value was size-adjusted to 1T (one-inch thickness) value based on the statistical weakest-link theory:

$$K_{Jc(1T)} = 20 + [K_{Jc(o)} - 20](\frac{B_0}{B_{1T}})^{1/4} \quad (2)$$

where:
$K_{Jc(1T)}$ = $K_{Jc}$ for a thickness of one inch ($B_{1T}$=25.4 mm),
$K_{Jc(o)}$ = $K_{Jc}$ for a specimen thickness of $B_o$.

To calculate the Master Curve provisional reference temperature $T_{oQ}$, the multi-temperature analysis equation in Eq. (3) was applied, and $K_{Jc}$ data were censored against both the fracture toughness capacity limit $K_{Jclimit}$ and the slow stable crack growth limit $K_{Jc\Delta a}$.

$$\sum_{i=1}^{N} \delta_i \frac{\exp[0.019(T_i - T_{oQ})]}{11.0 + 77\exp[0.019(T_i - T_{oQ})]} - \sum_{i=1}^{N} \frac{(K_{Jc(i)} - 20)^4 \exp[0.019(T_i - T_{oQ})]}{\{11.0 + 77\exp[0.019(T_i - T_{oQ})]\}^5} = 0 \quad (3)$$

$$K_{Jclimit} = \sqrt{\frac{Eb_o\sigma_{YS}}{30(1-\nu^2)}} \quad (4)$$

where:
N = number of specimens tested,
$T_i$ = test temperature corresponding to $K_{Jc(i)}$,
$K_{Jc(i)}$ = either a valid $K_{Jc}$ datum or a datum replaced with a censoring value,
$\delta_i$ = 1.0 if the datum is valid or 0 if the datum is a censored value,
$T_{oQ}$ = Master Curve provisional reference temperature solved iteratively,
$E$ = Young's modulus at the test temperature,
$b_0$ = initial uncracked ligament size,
$\sigma_{YS}$ = yield strength at the test temperature,
$\nu$ = Poisson's ratio ($\nu$=0.3).

## 3. RESULTS AND DISCUSSION

### 3.1 Specimen Size and Geometry Effects on $T_{0Q}$

The transition fracture toughness results of EUROFER97 batch-3 and F82H-BA12 from three specimen geometries are shown in Figs. 2 and 3, respectively. From Eq. (3), we calculated the Master Curve provisional reference temperature, $T_{oQ}$, and then the Master Curves were plotted in Figs. 2 and 3 using the following equation:

$$K_{Jc(med)} = 30 + 70\exp[0.019(T - T_{oQ})] \quad (5)$$

where:
$K_{Jc(med)}$ = median fracture toughness for a multi-temperature data set of 1T specimens,
T = test temperature,
$T_{oQ}$ = Master Curve provisional reference temperature.

Also shown in the same figures are the fracture toughness capacity limits $K_{Jclimit}$ calculated from Eq. (4) and the tolerance bounds calculated using the equation below:

$$K_{Jc(0.xx)} = 20 + [\ln(\frac{1}{1-0.xx})]^{1/4}\{11 + 77\exp[0.019(T - T_{oQ})]\} \quad (6)$$

where:
0.xx = selected cumulative probability level, e.g., for the 2% tolerance bound, 0.xx=0.02.

As shown in Figs 2 and 3, most valid data were bounded by the tolerance bounds indicating that the experimental fracture toughness results were within the statistical predictions of the Master Curve method. The testing temperatures for 0.5T CT and 4 mm miniCT specimens were within the ±50°C limit from the derived $T_{0Q}$, while the testing temperatures for the 1.65 mm bend bar were more than 50°C lower than the derived $T_{0Q}$ due to the low $K_{Jclimit}$ of the bend bar. The derived $T_{0Q}$ from three specimen geometries for the EUROFER97 batch-3 and F82H-BA12 are compared in Fig. 4. Within ±one standard deviation (±1σ) and for the same specimen type, $T_{0Q}$ was similar between EUROFER97 batch-3 and F82H-BA12. However, for both materials, $T_{0Q}$ from 1.65 mm bend bar specimens were higher than $T_{0Q}$ from 0.5T CT and 4 mm miniCT specimens. This observation contradicts earlier results reported in [17, 18] and needs to be evaluated further. For both materials, the particular heats tested in this study have not been tested by other investigators therefore no comparison with literature data can be made during the preparation of this manuscript.

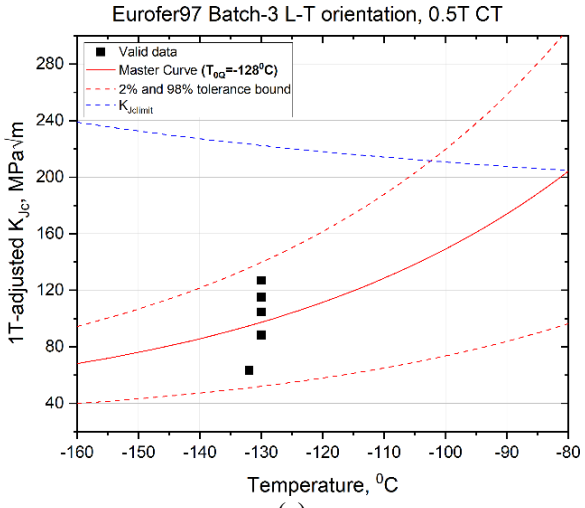

(a)

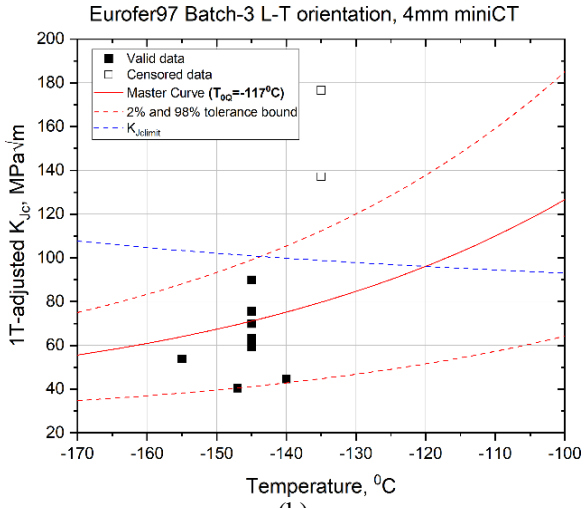


(b)

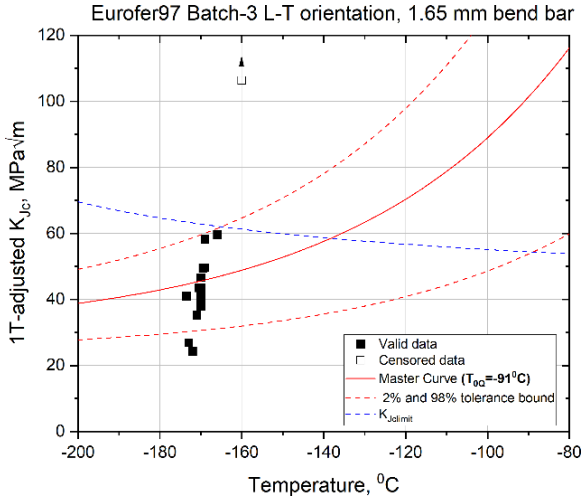


(c)

**FIGURE 2:** Master curve fracture toughness results for EUROFER97 (a) 0.5T CT, (b) 4 mm miniCT, and (c) 1.65 mm bend bar

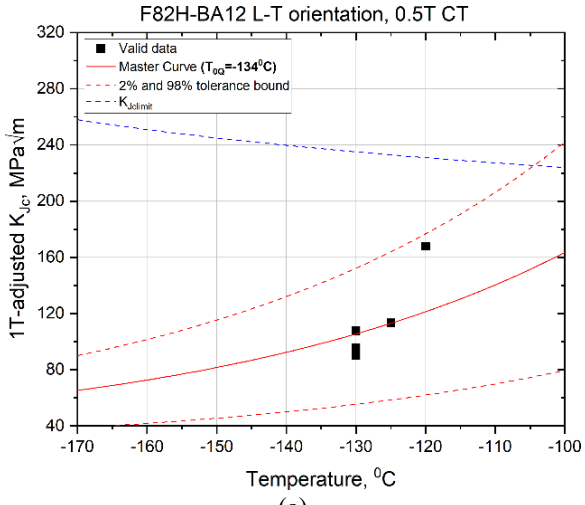


(a)

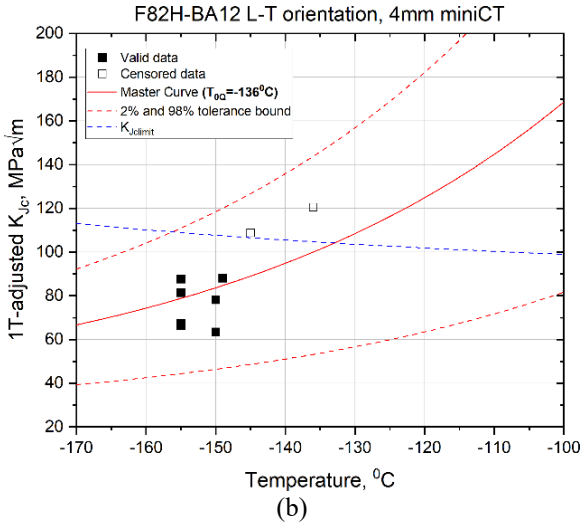


(b)

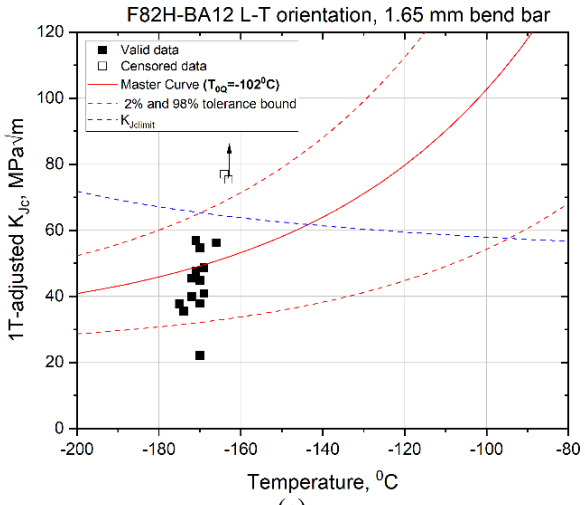


(c)

**FIGURE 3:** Master curve fracture toughness results for F82H-BA12 (a) 0.5T CT, (b) 4 mm miniCT, and (c) 1.65 mm bend bar

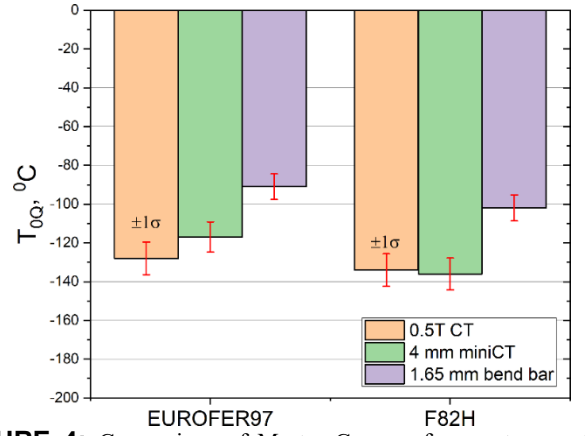


**FIGURE 4:** Comparison of Master Curve reference temperatures, $T_{0Q}$, between three specimen geometries for EUROFER97 batch-3 and F82H-BA12

### 3.2 Effect of Fatigue Precrack Front Straightness on $T_{0Q}$

In our first batch testing of 0.5T CT and 4 mm miniCT specimens, slanted fatigue precrack fronts were observed for both materials (Figs 5 and 6), while all 1.65 mm bend bar specimens yielded straight fatigue precrack front. It was later determined that a slight misalignment in the fatigue frame load train might have contributed to the slanted configuration of the fatigue precrack fronts. Therefore, improved alignment was achieved on the fatigue frame using preload spiral washers. In addition, for a few specimens, we also turned specimens around in relation to the fixture at the middle point of fatigue precracking [8]. Indeed, for the second batch testing of 0.5T CT and 4 mm miniCT specimens, we obtained reasonably straight fatigue precrack fronts as shown in Figs. 5 and 6 for EUROFER97 batch-3 and F82H-BA12, respectively. It is worth noting that the results presented in section 3.1 only came from the second batch of 0.5T CT and 4 mm miniCT specimen tests. One interesting observation for the first and second batch testing of 0.5T CT and 4 mm miniCT specimens is that $T_{0Q}$ was much lower for the 0.5T CT specimens with slanted fatigue precrack than for the specimens with straight fatigue precrack, whereas $T_{0Q}$ was not sensitive to the fatigue precrack front straightness in 4mm miniCT specimens. Specifically, $T_{0Q}$ was 40°C lower for EUROFER97 batch-3 and 15°C lower for F82H-BA12 when testing was performed on 0.5T CT specimens with slanted fatigue precracks. In contrast, $T_{0Q}$ was only 11°C lower for EUROFER97 batch-3 and 4°C higher for F82H-BA12 when testing was performed on 4 mm miniCT specimens with slanted fatigue precracks. One implication from this observation is that the smaller 4 mm miniCT specimens were less sensitive to test imperfections and yielded more consistent $T_{0Q}$ values. One possible explanation is that slanted fatigue precracks of 4 mm miniCT specimens had already extended from the machined notch for the entire specimen thickness (Fig. 5c and Fig. 6c) while that was not the case for 0.5T CT specimens as a small portion of the machined chevon notch remained intact (Fig. 5a and Fig. 6a). This would result in a different crack front stress field between 0.5T CT specimens and 4mm miniCT specimens during testing.

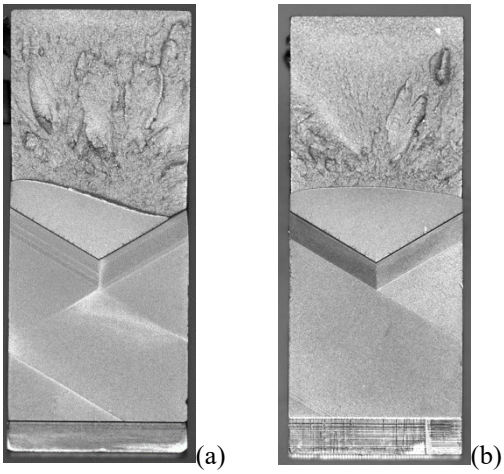
(a) (b)

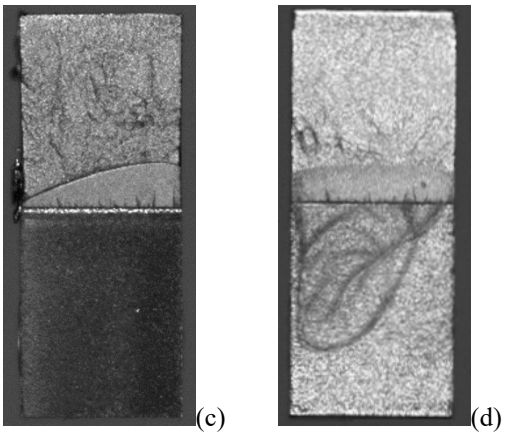
(c) (d)

**FIGURE 5:** Fracture surface images for EUROFER97 batch-3: (a) 0.5T CT with slanted fatigue precrack, (b) 0.5T CT with straight fatigue precrack, (c) 4 mm miniCT with slanted fatigue precrack, and (d) 4 mm miniCT with straight fatigue precrack

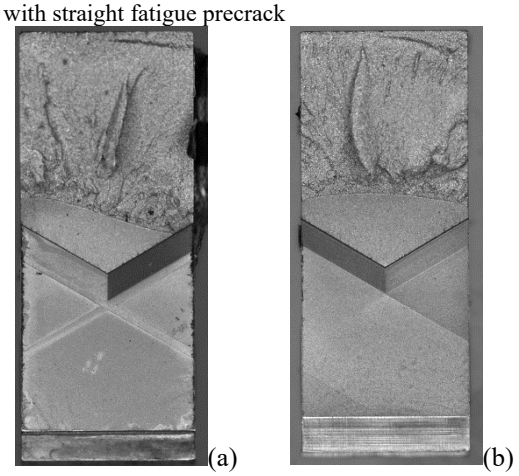
(a) (b)

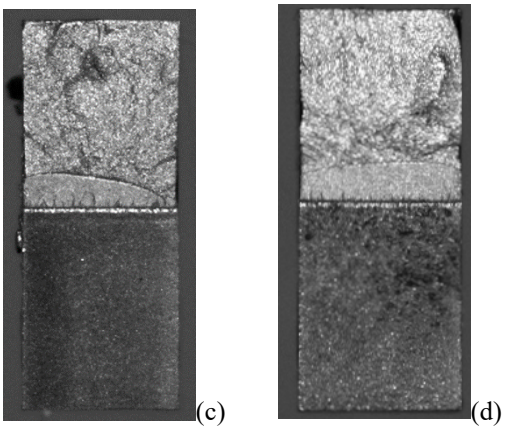
(c) (d)

**FIGURE 6:** Fracture surface images for F82H-BA12: (a) 0.5T CT with slanted fatigue precrack, (b) 0.5T CT with straight fatigue precrack, (c) 4 mm miniCT with slanted fatigue precrack, and (d) 4 mm miniCT with straight fatigue precrack

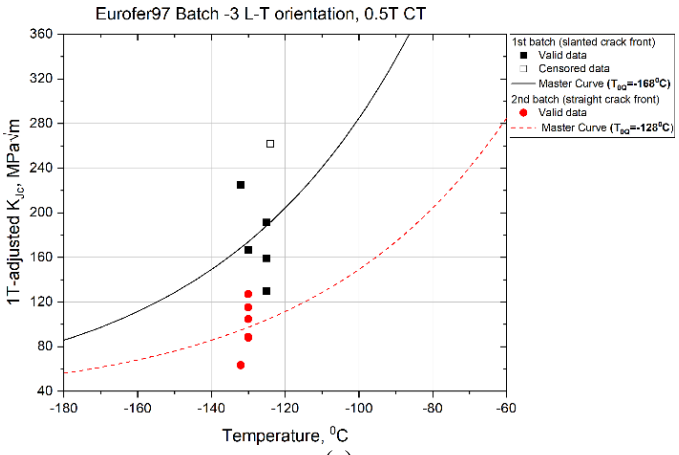


(a)

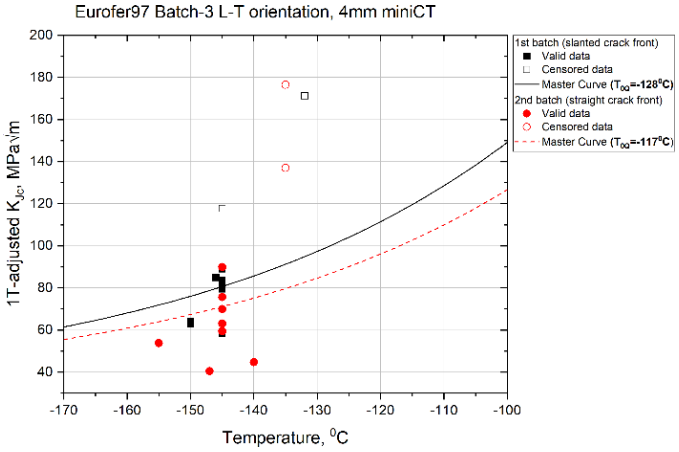


(b)

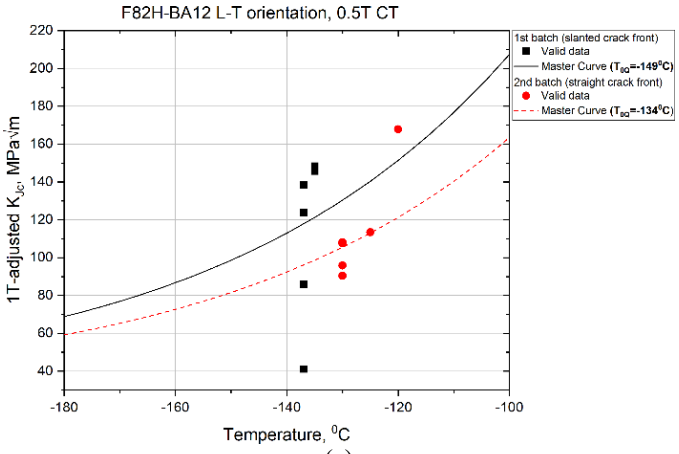


(c)

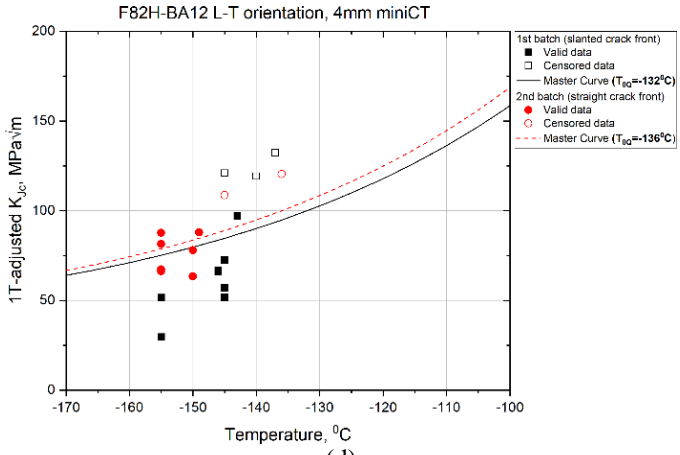


(d)

**FIGURE 7:** The effect of fatigue precrack front straightness for 0.5T CT and 4mm miniCT specimens on the Master Curve reference temperature, $T_{0Q}$, for EUROFER97 batch-3 in (a) and (b) and for F82H-BA12 in (c) and (d)

### 3.3 Determination of the Minimum Number of Specimens Required in Master Curve Testing

For experiment planning and materials qualification purposes, one important aspect of Master Curve fracture toughness characterization, especially for irradiated materials, is to determine the minimum number of specimens needed for evaluating $T_0$ for the specimen geometry. For both 0.5T CT and 4 mm miniCT specimens, testing and analysis can be performed in full compliance with the current ASTM E1921 standard, and the minimum number of specimens is shown in Table 2 according to ASTM E1921-19 [8].

**Table 2** Number of uncensored test results required to evaluate a valid $T_0$

| (T- $T_0$) range °C | 1T $K_{Jc(med)}$ range MPa√m | Number of uncensored tests required |
|---|---|---|
| 50 to -14 | 212 to 84 | 6 |
| -15 to -35 | 83 to 66 | 7 |
| -36 to -50 | 65 to 58 | 8 |

The situation is more complicated for the 1.65 mm bend bar specimens since 1T $K_{Jc(med)}$ from this specimen type is usually less than 58 MPa√m and the testing temperatures are more than 50°C lower than $T_{0Q}$, see Fig. 2c and Fig. 3c. Therefore, a new approach is proposed here. For both EUROFER97 batch-3 and F82H-BA12, 16 bend bars were tested in this study, with one test censored for EUROFER97 batch-3 and two tests censored for F82H-BA12. From the uncensored data, a randomized and smaller dataset can be used to calculate $T_{0Q}$. As the size of such dataset increases, the calculated $T_{0Q}$ would approach a constant value (referred to as $T_{0Qfinal}$ hereafter), corresponding to $T_{0Q}$ calculated with all uncensored data in this testing campaign (15 uncensored data for EUROFER97 batch-3 and 14 uncensored data for F82H-BA12). The minimum uncensored data for 1.65 mm bend bar specimens should correspond to the smallest

uncensored sample size such that for this sample size and beyond, the calculated $T_{0Q}$ should be within the $T_{0Qfinal}$ ± 1σ where the standard deviation, σ, was calculated as:

$$\sigma = \sqrt{\frac{\beta^2}{r} + \sigma_{exp}^2} \quad (7)$$

where:
β = sample size uncertainty factor, chosen as 20.1°C per ASTM E1921-19 standard,
r = total number of uncensored data used to establish the value of T0,
$\sigma_{exp}$ = contribution of experimental uncertainties, chosen as 4°C per ASTM E1921-19 standard,

Fig. 8 shows the $T_{0Q}$ range calculated from three randomized datasets for each designated number of uncensored data vs. the number of uncensored data for EUROFER97 batch-3 and F82H-BA12. Based on the aforementioned criterion, 12 uncensored data are needed for EUROFER97 batch-3 $T_{0Q}$ calculation and 10 are needed for F82H-BA12. For the sake of simplicity and conservatism, the minimum uncensored data for the evaluation of $T_{0Q}$ for 1.65 mm bend bar specimens are determined as 12 for EUROFER97 and F82H. This applies to a testing temperature range for T-$T_{0Q}$ from -50°C to -80°C.

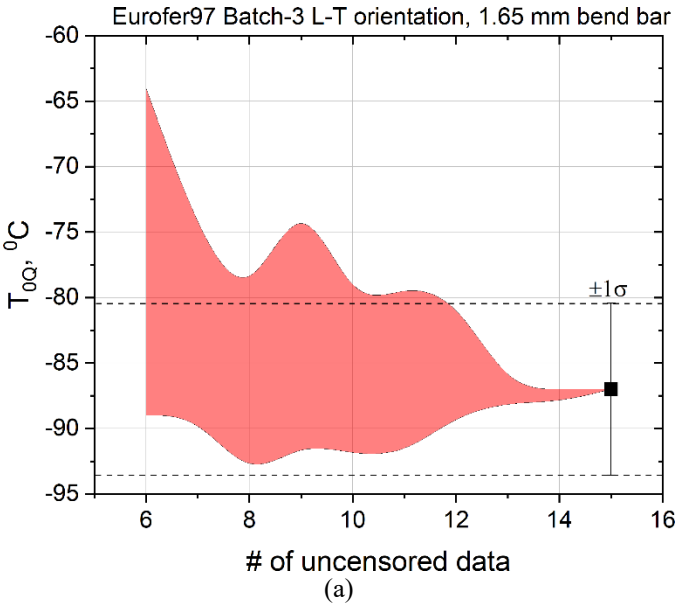

(a)

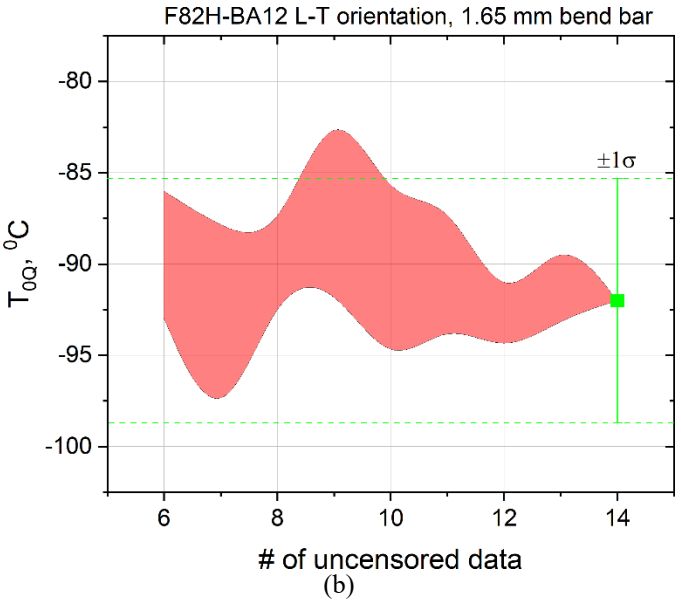

(b)

**FIGURE 8:** Effect of the number of uncensored tests in 1.65 mm bend bar testing on the determination of the Master Curve reference temperature $T_{0Q}$ for Eurofer97 batch-3 in (a) and F82H-BA12 in (b). Error bars correspond to ±1σ and the red overlays correspond to the $T_{0Q}$ range calculated from three randomized datasets for each designated number of uncensored tests.

## 4. CONCLUSION

EUROFER97 and F82H are two leading RAFM steels for fusion blanket applications. Commercialization of fusion technology requires an in-depth understanding of materials post-irradiation behavior, including FT properties, for the safe long-term operation of fusion reactors. Due to the space constraint of irradiation facilities, the development of SSTT is necessary to evaluate the performance of irradiated materials. In this study, we evaluated the specimen size and geometry effects on the Master Curve FT of EUROFER97 batch-3 and F82H-BA12 steels. The main findings are:

1) Considering ± one standard deviation (±1σ) and size correction to 1T size using the Master Curve method, there was no obvious specimen size effect in 0.5T CT and 4 mm miniCT specimens on measured Master Curve reference temperature $T_{0Q}$, while 1.65 mm bend bar specimens yielded a higher (more conservative) $T_{0Q}$ for both steels.
2) For the minimum number of specimens needed for evaluating the Master Curve reference temperature $T_{0Q}$, ASTM E1921 can be used for 0.5T CT and 4 mm miniCT specimens, while, for 1.65 mm bend bar specimens, 12 uncensored tests would be required for EUROFER97 and F82H.
3) Experimental quality control is critical for generating valid Master Curve results. Small misalignments in fatigue precracking can result in slanted fatigue precrack fronts in 0.5T CT and 4 mm miniCT specimens. In that regard, 0.5T CT specimens with slanted fatigue precrack fronts yielded a much lower $T_{0Q}$ than the specimens with straight fatigue

precrack fronts, whereas 4mm miniCT specimens are less sensitive to fatigue precrack front straightness.

## ACKNOWLEDGEMENTS

This research was sponsored by the U.S. Department of Energy, Office of Fusion Energy Sciences, under contract DE-AC05-00OR22725 with UT-Battelle, LLC. We also appreciate the support from the IAEA CRP F13017 “Towards the Standardization of Small Specimen Test Techniques for Fusion Applications”. The views and opinions expressed herein do not necessarily reflect those of the International Atomic Energy Agency. The raw materials used in this study, EUROFER97 Batch 3 and F82H BA12, were provided by Fusion for Energy (F4E) and National Institutes for Quantum and Radiological Science and Technology (QST), respectively.

We appreciate contributions from the following personnel at ORNL: Eric Manneschmidt and Jordan Reed for performing fracture toughness testing; Doug Stringfield for facilitating specimen machining. Lastly, we would like to thank Tim Graening and TS Byun, also from ORNL, for their thoughtful review of this manuscript before publication.

## REFERENCES

[1] Shiba, K., Tanigawa, H., Hirose, T., and Nakata, T., 2012, "Development of the toughness-improved reduced-activation F82H steel for DEMO reactor," Fusion Science and Technology, 62(1), pp. 145-149.

[2] Tan, L., Katoh, Y., Tavassoli, A.-A., Henry, J., Rieth, M., Sakasegawa, H., Tanigawa, H., and Huang, Q., 2016, "Recent status and improvement of reduced-activation ferritic-martensitic steels for high-temperature service," Journal of Nuclear Materials, 479, pp. 515-523.

[3] Shiba, K., Enoeda, M., and Jitsukawa, S., 2004, "Reduced activation martensitic steels as a structural material for ITER test blanket," Journal of nuclear materials, 329, pp. 243-247.

[4] Jitsukawa, S., Tamura, M., Van der Schaaf, B., Klueh, R., Alamo, A., Petersen, C., Schirra, M., Spaetig, P., Odette, G., and Tavassoli, A., 2002, "Development of an extensive database of mechanical and physical properties for reduced-activation martensitic steel F82H," Journal of Nuclear Materials, 307, pp. 179-186.

[5] Tavassoli, A.-A., Rensman, J.-W., Schirra, M., and Shiba, K., 2002, "Materials design data for reduced activation martensitic steel type F82H," Fusion Engineering and Design, 61, pp. 617-628.

[6] Garner, F., and Greenwood, L., 1998, "Neutron irradiation effects in fusion or spallation structural materials: some recent insights related to neutron spectra," Radiation effects and defects in solids, 144(1-4), pp. 251-286.

[7] González de Vicente, S. M., Boutard, J. L., Zinkle, S. J., and Tanigawa, H., 2017, "Materials testing facilities and programmes for fission and ion implantation damage," Nuclear Fusion, 57(9), p. 092011.

[8] ASTM, 2019, "ASTM E1921-19 Standard Test Method for Determination of Reference Temperature, To, for Ferritic Steels in the Transition Range," ASTM International, West Conshohocken, PA, p. 39.

[9] Möslang, A., Diegele, E., Klimiankou, M., Lässer, R., Lindau, R., Lucon, E., Materna-Morris, E., Petersen, C., Pippan, R., and Rensman, J., 2005, "Towards reduced activation structural materials data for fusion DEMO reactors," Nuclear fusion, 45(7), p. 649.

[10] Commin, L., Baumgärtner, S., Dafferner, B., Heger, S., Rieth, M., and Möslang, A., 2014, "Creep-Fatigue Interaction in Eurofer 3 Electron Beam Welds," Fusion Science and Technology, 66(1), pp. 131-135.

[11] Chen, X., Hernandez Pascual, R., Serrano, M., Andres, D., Nolles, H., and Sokolov, M. A., 2020, "Guidelines for IAEA Small Specimen Test Techniques Master Curve Fracture Toughness Testing," United States. doi:10.2172/1649107.

[12] Chen, X., Sokolov, M. A., Bhattacharya, A., Clowers, L. N., Graening, T., Katoh, Y., and Rieth, M., "Master Curve Fracture Toughness Characterization of Eurofer97 Steel Variants Using Miniature Multi-Notch Bend Bar Specimens for Fusion Applications," Proc. ASME 2019 Pressure Vessels & Piping Conference V001T01A036. https://doi.org/10.1115/PVP2019-93797.

[13] Chen, X., Sokolov, M. A., Katoh, Y., Rieth, M., and Clowers, L. N., "Master Curve Fracture Toughness Characterization of Eurofer97 Using Miniature Multi-Notch Bend Bar Specimens for Fusion Applications," Proc. ASME 2018 Pressure Vessels and Piping Conference V01AT01A076. https://doi.org/10.1115/PVP2018-85065.

[14] Chen, X., Sokolov, M. A., Linton, K. D., Clowers, L. N., and Katoh, Y., 2017, "Transition Fracture Toughness Characterization of Eurofer 97 Steel using Pre-Cracked Miniature Multi-notch Bend Bar Specimens," United States. doi:10.2172/1414686.

[15] Chen, X., Bhattacharya, A., Sokolov, M. A., Clowers, L. N., Yamamoto, Y., Graening, T., Linton, K. D., Katoh, Y., and Rieth, M., 2019, "Mechanical properties and microstructure characterization of Eurofer97 steel variants in EUROfusion program," Fusion Engineering and Design, 146, pp. 2227-2232.

[16] Chen, X. F., Sokolov, M. A., Robertson, J., Ando, M., Geringer, J. W., Tanigawa, H., and Katoh, Y., 2020, "Effects of HFIR neutron irradiation on fracture toughness properties of standard and Ni-doped F82H," Journal of Nuclear Materials, 542, p. 152501.

[17] Sokolov, M., and Tanigawa, H., 2002, "Fusion Reactor Materials Program Semiannual Progress Report."

[18] Sokolov, M., and Tanigawa, H., 2006, "Fusion Reactor Materials Program Semiannual Progress Report."

---

for US government purposes. DOE will provide public access to these results of federally sponsored research in accordance with the DOE Public Access Plan (http://energy.gov/downloads/doe-public-access-plan).